Hindawi
Journal of Chemistry
Volume 2022, Article ID 9034840, 12 pages
https://doi.org/10.1155/2022/9034840

Research Article

Biogenic Synthesis of Gold Nanoparticles from *Physalis peruviana* and Application in Wound Healing

Stephen Adongo Odongo,[1] **Fredrick Oluoch Okumu**,[1] **Solomon Omwoma Lugasi**,[1] **Martin Opiyo Onani**,[1] **and Stephen Gaya Agong**[2]

[1]*Department of Physical Sciences, Jaramogi Oginga Odinga University of Science and Technology, P. O. Box 210-40601, Bondo, Kenya*
[2]*Department of Plant, Animal and Food Sciences, Jaramogi Oginga Odinga University of Science and Technology, P. O. Box 210-40601, Bondo, Kenya*

Correspondence should be addressed to Solomon Omwoma Lugasi; solomwoma@yahoo.com

Received 10 February 2022; Accepted 4 July 2022; Published 12 September 2022

Academic Editor: Samuel Lalthazuala Rokhum

Wound management is key to healing. Poorly managed wounds lead to abnormal biological reactions and complications. Microorganisms, bacteria or fungi, infect such wounds leading to their chronic nature. Gold nanoparticles (Au NPs) show wound healing properties. In addition, ethnobotanical information from Siaya County in Kenya shows the leaves of *Physalis peruviana* L. to be effective in wound management. A combination of Au NPs and leave extracts of *Physalis peruviana* L. through a one pot biogenic synthesis leads to a new effective wound management substance. The synthesis was done at room temperature 25°C and at 85°C. The UV-visible spectroscopy results show efficient sharper plasmon bands with a blue shift indicating a decrease in λ max compared to red shift which show an increase in λ max. The surface plasmon resonance is a sharper at wavelength of about 540 nm. Dynamic light scattering and zeta potential analysis show that the polydispersity index is high and this is attributed to heterogeneity of chemical components of the plants. Transmission electron microscopy results for Au NPs show similarity in their shapes and sizes with grain size boundaries of between 1 nm and 100 nm. The particles are spherically shaped and crystalline with small lattice due to the small grains. The gold nanoparticles synthesized from *Physalis peruviana* show antimicrobial activities against gram-positive bacteria and, gram-negative bacteria as well as gram-positive fungus. The inhibition zones for Au NPs of different concentrations vary significantly between concentrations (one-way ANOVA at $P < 0.05$). The highest antibacterial activity is at 100 mM of Au NPs against *Escherichia coli, Bacillus subtilis,* and *Staphylococcus aureus*. The inhibition zones for Au NPs at concentration of 100 mM and *Physalis peruviana* extract vary significantly in all the microbial cells, except for *Pseudomonas aeruginosa* (one-way ANOVA, $F_{(3,11)} = 2.67$, $P = 0.1189$). Application of the Au NPs in wound healing is faster than controls. The Au NPs also have good biocompatibility as signs of infection were not present.

1. Introduction

The human skin is considered key to our survival: sensing the environment; maintaining physicochemical and thermal homeostasis: being a reservoir of essential nutrients; providing passive and active defense; responding to trauma and injury, etc. [1]. When the skin is injured, it results into a wound. Management of wounds has been a challenge to mankind. There are two specific types of wounds: chronic and acute wounds [2]. Chronic wounds are considered silently epidemic and possess serious threat towards public health and global economy [3]. They do not heal within a predictable period of time, leading to further complications due to infections and difficulty in healing [4]. Examples of such wounds include diabetic ulcers, vascular ulcers, and pressure ulcers. For the case of acute wounds, they are caused by incisions and are with patients who pass through surgical treatments, traumas, abrasions, or epithelial burns [5].

Wounds are susceptible to infection due to breakage of cutaneous barrier that protects the underlying tissue against

microorganisms such as *S. aureus, P. aeruginosa, E. coli,* and *Streptococci* [6]. The extent of infection depends on the degree of pathogenicity of the invading organisms and the ability of the host to defend itself [4]. The healing process is divided into four important phases; coagulation (haemostasis), inflammation, proliferation (granulation), and remodelling (maturation) [7].

Wound dressings containing plant extract with antimicrobial compounds can be applied in order to control wound infections. Wound infections can be caused by planktonic bacteria, biofilms, and fungus. It is essential to determine whether the plant extract loaded wound dressing has an effect on these species or not [8]. Wound therapy has moved from drying out the wound bed to maintaining a balanced moist environment [9]. Traditional dressings involve absorbing wound exudate and this made the wound to develop a crust on its surface with remarkable scarring. This has since been replaced by modern dressings which aim at improving healing by handling wound fluid in a way that prevents accumulation of excess exudate while maintaining a certain degree of moisture, and thereby enhancing the chance of obtaining new skin tissue without scarring [10]. There has been a constant search for methods and materials which can help in reducing the quantity of scar tissue and, ultimately, its remodelling and hence a great progress in the preparation of engineered nanoparticles for different biological applications [11]. This has made researchers to exploit biological synthesis of nanoparticles using plant extracts [12–14].

The importance of gold nanoparticles (Au NPs) ranges from chemical stability, capacity to absorb infrared light, ease of synthesis and applications in wound therapy [15]. Several polymeric, lipid-based, ceramic, inorganic, metal, and metal oxide nanomaterials have been widely investigated for cutaneous wound healing [16]. According to a research study by Arafa and El-Kased [17], the surface plasmon resonance is tuned to make the Au NP gels gain thermo responsiveness, and this improves the NP antibacterial and healing properties, both in-vitro and in-vivo, a fact backed by histopathologic examinations [17].

Gold NPs can either directly target the bacterial cell wall or can bind to bacterial DNA, blocking the double-helix from uncoiling during replication or transcription, thus exerting bactericidal and bacteriostatic properties. As a result, they can inhibit multidrug-resistant pathogens, such as *S. aureus* and *P. aeruginosa*. Moreover, Au NPs prevent the formation of reactive oxygen species, thus acting as antioxidants, aiding the healing process [18]. A study on ex vivo permeation showed that gold NPs can also be used in the therapy of burns, being able to promote healing and inhibit microbial colonization, while being transdermally active [17]. It has been reported that interaction of inorganic nanoparticles and gold nanoparticles for this matter with microorganisms may exhibit antibacterial and antifungal activity [19]. The gold nanoparticles exhibit strong cytotoxicity to varied microorganisms; the interaction with various surface-exposed functional groups present on the bacterial cell surface may lead to bacterium destruction and inactivation. This activity may either be as a result of coating on the Au NPs surface or to reaction contaminants left over from the manufacturing approach rather than the Au NPs cores [20].

2. Material and Methods

Hydrochloric acid, sodium hydroxide, and hydrogen tetrachloroaurate (III) were purchased from Sigma-Aldrich, South Africa. Autoclaved distilled water was used throughout the experiments. Eppendorf tubes of 1.5 mL were used for optimization. The ethical review number at Jaramogi Oginga Odinga University of Science and Technology is ERC/29/4/22–25 with a subsequent research permit from the National Commission for Science, Technology and Innovation, Kenya identification license number: NACOSTI/P/22/18037 (see support information file). The recommended small animal handling certificate by the ethical review committee was done at the Jomo Kenyatta University of Agriculture and Technology (support information file).

2.1. Collection of Plant Materials. Plant materials, *Physalis peruviana* L. (see Figure 1), used for the study were collected from Gem Subcounty which is located in Siaya County in Kenya. Siaya County lies between latitude 0°26′ and 0°18′ north and longitude 33°58′ east and 34°33′ east [21]. The climate of the study area is heavily influenced by its geographical location and altitude relative to the Lake Victoria. The study area stands in the upper eastern flanks of Lake Victoria, therefore benefiting from the convergence of the easterlies and lake winds. The samples were taken from April to end of July at different places within a radius of 100 meters in 2019. Leaves from these plants were harvested and kept in brown paper envelopes for transportation to the laboratory.

2.2. Synthesis and Characterization of Au NPs. Synthesis and characterization of gold nanoparticles were done according to Kumar et al. [22]. They are described fully in the support information. Synthesis was done for 1 hour both at room temperature (25°C). Colour changes were observed whereby a ruby red or a red wine colour was desired. The 96-well plate was used to determine the absorbance for the reaction. An efficient surface plasma resonance (SPR) was studied based on the peaks obtained using ultraviolet-visible spectroscope (Polar Star Omega, BMG LABTECH GmbH, 77656, Ortenberg, Germany). This informed the choice of synthesis conditions for the gold nanoparticles.

2.3. Characterization Studies. Ultraviolet-visible spectroscopy (UV-Vis) was performed using UV-visible spectrophotometer (Polar Star Omega, BMG LABTECH GmbH, 77656, Ortenberg/Germany) in a range of 400–700 nm. The studies of size and morphology of the nanoparticles were performed using transmission electron spectroscopy (TEM) in the Physics Department, University of Western Cape, and surface area electron dispersion (SAED) using FEI Tecnai G2 20 field-emission gun. Samples for TEM studies were

Figure 1: *Physalis peruviana* L. (cape gooseberry); family: Solanaceae.

prepared by placing drops of the Au NPs on carbon-coated TEM copper grids. Dynamic light scattering (DLS) was used to determine the zeta potential of the synthesized Au NPs. The hydrodynamic diameter of the Au NPs was calculated by the Stokes–Einstein equation in which water was used as a continuous phase. The polydispersity index (PDI) measured the molecular mass distribution of the synthesized nanoparticles.

2.4. In-Vitro Studies of Gold Nanoparticles. The interaction between gold nanoparticles against various kinds of pathogenic microorganisms was studied. The experimental studies involved the measurements of the mortality constant rate for various gram-negative and gram-positive bacterial strains from the American Type Culture Collection (ATCC) as well as fungal strains; *E. coli* (ATCC, 10536), *P. aeruginosa, C. albicans,* and *B. subtilis* (ATCC, 6538). The agar solution was incubated for 24 hours at 37°C after sterilization. The inhibition zone was measured after 24 hours of incubation by the disc diffusion method that was performed on Mueller–Hinton agar. To ensure reproducibility, the experiment was repeated three times. The minimum inhibitory concentration (MIC) and the minimum bactericidal concentration (MBC) were also obtained using *E. coli* (ATCC, 8739), *E. faecalis*, *S. aureus* (ATCC, 6538), and *S. saprophyticus* in nutrient agar medium after 24 hours of incubation [23].

2.5. Inoculation of Microorganism. The nutrient agar medium was prepared by dissolving 28 g of nutrient agar in 1000 mL of hot distilled water and allowed to cool. The mixture was then sterilized by autoclaving at 120°C for about 15 min at 15 psi pressure and cooled to 50°C [23]. The medium was dispensed into Petri-dishes to yield a depth of 4 mm and isolated colonies were aseptically transferred to nutrient broth in the Petri-dishes and incubated at 37°C for 24 hours so as to mimic human body temperature since the bacteria that were used are human pathogens.

2.6. Sample Preparation. Minimum inhibitory concentration (MIC) of Au NPs for various concentrations (range: 100–0.01 mM) was tested [23]. Disks of 6 mm were placed in solutions of gold nanoparticles prepared from different concentrations of gold salt. The disks were screened for anti-*E. coli,* anti-*S. aureus*, anti-*P. aeruginosa,* anti-*C. albicans,* and anti-*B. subtilis* activities by using disc diffusion method in Botany Department, J.K.U.A.T [23]. Inoculum suspension (108 CFU/Ml) was spread over the nutrient agar surface by sterile collection swab and 6 mm disc was sterilized at 120°C for about 15 min and then loaded with gentamycin (10 mg/mL) each as positive controls. The films were placed onto the surface of inoculated plates with flamed forceps. The plates were labeled and incubated at 37°C for 24 hours for 2–3 days. The zone of inhibition (ZOI) was measured using a ruler in millimeters around the disc as low activity (1–6 mm), moderate activity (7–10 mm), high activity (11–15 mm), very high activity (16 and above), and no activity (0) [24].

2.7. In-Vitro Disc Diffusion Antimicrobial Assays. The interaction between gold nanoparticles against various kinds of microorganisms was studied using disc diffusion assays. The experimental studies were focused on the measurements of the mortality constant rate for *E. coli* (ATCC, 10536), *S. aureus* (ATCC, 6538), *P. aeruginosa, C. albicans,* and *B. subtilis.* The agar solution was incubated for 24 h at 37°C after sterilization [25]. The zones of inhibition were measured after incubation of 6 mm disk impregnated with Au NPs for 24 h on Mueller–Hinton agar. To ensure reproducibility, the experiments were carried out three times and the zones of inhibition reported as the mean ± standard deviation. The minimum inhibitory concentrations (MIC) were obtained using Au NPs prepared using different concentrations [25].

2.8. In-Vivo Wound Healing Studies. To evaluate the wound healing properties of Au NPs, a nude rabbit with no hair on the skin was used [7]. (Training in small animal handling was done at JKUAT in collaboration with JICA). Using a cotton swab, part of the back was scrubbed off by rubbing a depilatory on the epidermis of the skin and incising a wound 2 cm in length using a scalpel blade. This procedure was carefully carried out to avoid damaging the subcutaneous tissue under the dermis. Before placing the bandage on the prepared wound, the Au NPs were applied on the sterile cotton swabs by deep coating the gauze in the nanoparticle's solution for 1 hr followed by drying in an oven set at 50°C to constant weight. The Au NP coated gauze was then stuck on the wounded part and the healing condition was observed for 14 days [26].

3. Results and Discussion

Temperature, time, pH, and concentration of the plant extracts as well as concentration ratio of the gold salt to the plant extracts were optimized. The concentration of hydrogen tetrachloroaurate (III) was 1 mM. Aqueous leaf extract of *Physalis peruviana* was used for optimization and synthesis. The formation of the ruby red colour was an indication that synthesis had taken place.

3.1. Au Nanoparticle Synthesis. Synthesis of Au NPs to determine the optimum ratio of the gold salt to the plant extract was done with 1 mM $HAuCl_4$, for the duration of 60 minutes at varied ratio of hydrogen tetrachloroaurate (III) and the aqueous leaf extract of the plant. Choice of 1 mM was from a similar study that optimized synthesis parameters and found that 1 mM concentration of $HAuCl_4$ was suitable for biogenic synthesis [27]. The formation of the ruby red colour was attributed to successful synthesis of Au NPs because of the presence of polyphenolic content and radical scavenging ability of the plant extract [28]. The phenolic compounds present in polyphenols serve as both reducing and capping agents by forming complexes with the metal ions, reducing them to nanoparticles of diverse sizes and morphologies [29–31]. The change in colour of the solution was observed within 20–30 min and the reaction was allowed to proceed for 60 minutes. The UV-Vis spectroscope was further used to characterise the synthesized gold nanoparticles. The UV-Vis spectra revealed the presence of the SPR band of the Au NPs at a wavelength of approximately 540 nm. Transmission electron spectroscopy (TEM) was further used to confirm the analysis by UV-Vis spectroscopy which suggested that the biogenically synthesized Au NPs were likely to be anisotropic in shape as well as size.

3.2. Au Nanoparticle Characterization. Characterization was done on the synthesized Au NPs using UV-Vis spectroscopy at room temperature (Figure 1). It was also used to estimate the size, shape, and concentration of the Au NPs by observing their optical intensity through the surface plasmon resonance (SPR) effect which gives rise to an absorption band at a wavelength ranging from 400 to 700 nm [32]. The surface plasmon resonance wavelength of Au NPs is mainly dependent on the size of individual Au NPs and the aggregation state of the Au NPs [33]. The UV-Vis spectra of the Au NPs are affected by various factors including the size, shape, and concentration of the nanoparticle [34]. The standard SPR of gold is between wavelengths 500–550 nm [35]. The UV-Vis spectra revealed the presence of the SPR band of the Au NPs at approximately 540 nm. This is in agreement with previous research [36, 37]. The presence of the SPR band was as a result of collective oscillations of the free electrons caused by an interacting electromagnetic field in metallic NPs [38].

The synthesis of Au NPs at room temperature (25°C) with a 2 : 1 ratio of hydrochloroauric acid trihydrate to the plant extract was observed to provide efficient sharper plasmon bands with a blue shift (indicated by decrease in λ max) compared to the synthesis at higher concentration ratio showing values as well as higher concentration of plant extract compared to the gold salt, leading to a red shift (indicated by increase in λ max). Higher concentrations show concentration values leading to instability of the Au NPs and this may have affected capping agents and hence formation of less anisotropic Au NPs. This temperature dependent correlation was also reported in various other studies [39, 40] while the effect of concentration on size of particles was also reported in other studies [41]. Further optimization showed that plant concentration of 17.5 mg/ml and pH of 9 were more viable for synthesis. However, in another study, pH 7, 8, and 12 showed characteristic absorption during biogenic synthesis of gold nanoparticles [42]. This reaction was timed for 1 hr and synthesis took 50 minutes to reach a completion. Similar synthesis reactions took 120 to 150 mins though some syntheses would take as low as 10 minutes [42]. Other than room temperature synthesis, another synthesis was also carried out with temperature ranging between 25°C and 85°C.

Temperature of 85°C was found to be the most viable for the synthesis within the selected temperature range (Figure 2(b)). UV-visible spectroscopy is used to estimate the size, shape. And concentration of the Au NPs by observing their optical intensity through the SPR effect which gives rise to an absorption band at a wavelength ranging from 400 to 700 nm [32]. The Beer–Lambert law is applied where a beam of monochromatic light is passed through a solution of an absorbing substance and the intensity of radiation monitored. The rate of decrease of intensity of radiation with thickness of the absorbing solution is proportional to the incident radiation and the concentration of the solution. The resultant Au NPs from the optimum concentrations of *Physalis peruviana* L. plant extracts were chosen for further study and their UV-Vis spectra results provided. The UV-Vis spectra of the Au NPs are affected by various factors including the size, shape, and concentration of the nanoparticle [34].

Synthesis at low temperatures may favour synthesis unlike in high temperatures. This could be due to the unique properties of the phytochemicals present in the plant, which react differently with the gold salt under the specific conditions. Moreover, it could also be postulated that the sensitive phytochemicals could be destructed by some heat which affects the synthesis of Au NPs. Higher temperature is believed to alter the interaction of phytochemicals with the nanoparticle surface, thereby inhibiting incorporation of adjacent nanoparticles into the structure of nanoribbons. Furthermore, in some situations, higher temperatures may facilitate the nucleation process to the detriment of the secondary reduction process and further condensation of a metal on the surface of nascent nanoparticles [43].

Dynamic light scattering (DLS) and zeta potential showed that the PDI was high and this may be attributed to the heterogeneity of the chemical components of the plants. Figure 3 shows the size distribution histogram by intensity from zeta potential for synthesized Au NPs using *Physalis peruviana* plant extract at room temperature.

It is observed from the histogram that the highest single peak is between 10 nm and 100 nm. This shows that after reaching a peak point, the scattering light intensity actually decreases. Some of the laser light is absorbed or scattered by the sample before the beam reaches the scattering volume, thereby decreasing the laser intensity at the scattering volume and reducing the amount of light available for scattering in the scattering volume. Likewise, light scattered from the scattering volume is absorbed or rescattered by the

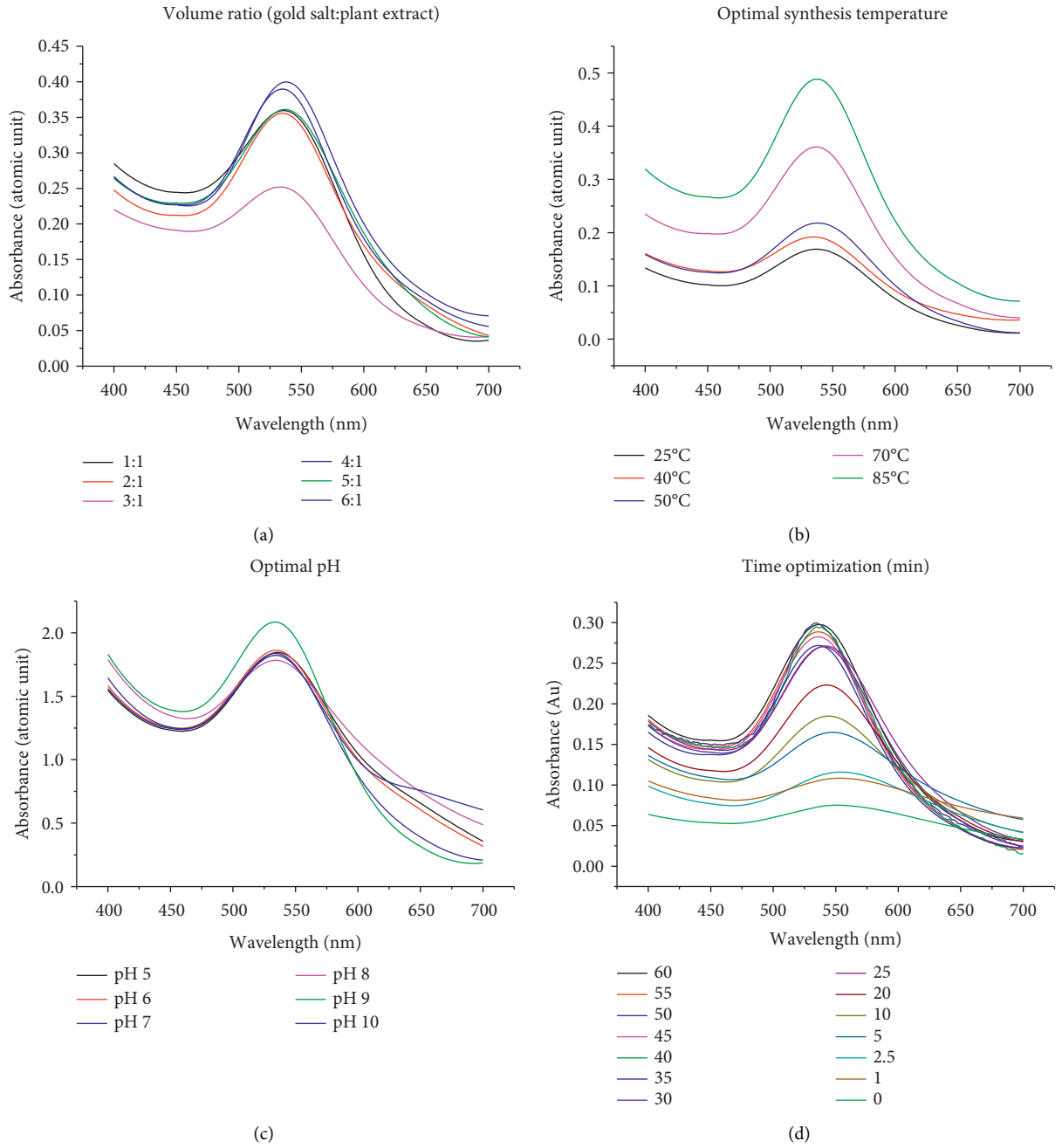

Figure 2: UV-Vis spectra for (a) concentration course, (b) temperature course, (c) pH course, and (d) time course for synthesis using *Physalis peruviana*.

medium on the way to the detector, thereby also decreasing the amount of scattered light reaching the detector [44].

Transmission electron microscopy as technique is used to show the morphology and the shape of the synthesized nanoparticles. In this research study, spherical shapes are more dominant with room temperature synthesis. There is a diversity in the geometrical shapes of green synthesized Au NPs [40, 45]. The anisotropic nature of the synthesized Au NPs as shown by TEM confirms the analysis done by UV-Vis which suggested that the Au NPs synthesized from *Physalis peruviana* plant extract are likely to be anisotropic in shape and size. Figure 4 shows the TEM images and the SAED for room temperature synthesis, i.e., Figures 4(a) and 4(b), as well as synthesis at 85°C, i.e., Figures 4(c) and 4(d), respectively.

The Au NPs are porous and have a hollow structure. The grain boundaries are of size 10 nm. The smaller the grains, many pores could lead to large surface area. The particles are also crystalline and the small lattice is due to the small grains. Room temperature synthesis resulted in spherical-shaped

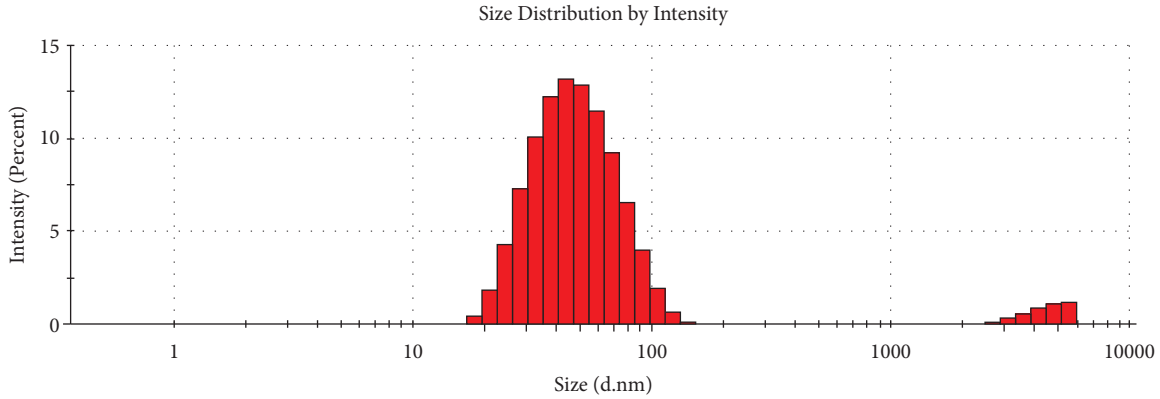

Figure 3: Size distribution against intensity histogram from zeta potential for room temperature synthesized Au NPs using *Physalis peruviana*.

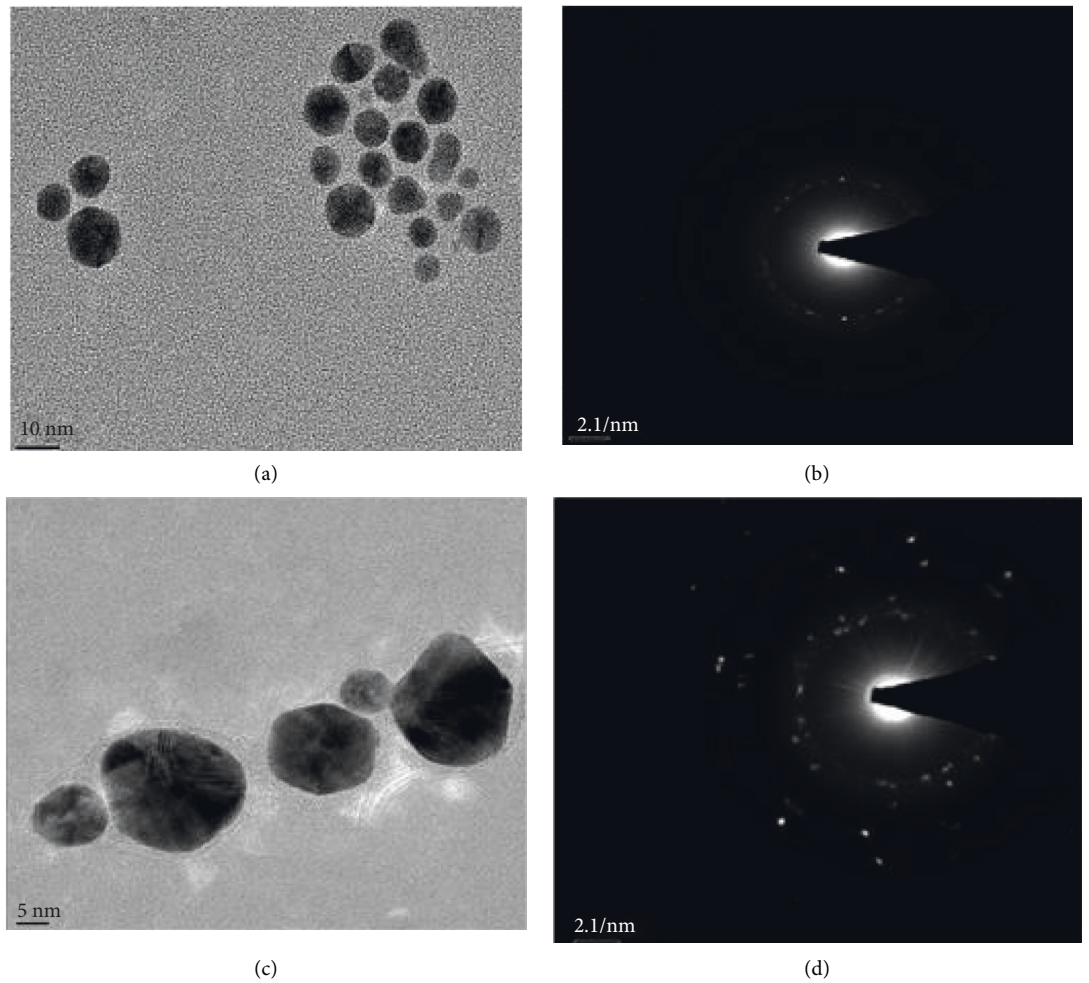

Figure 4: The TEM images and the SAED for room temperature synthesis (a, b), as well as synthesis at 85°C (c, d).

Au NPs which are equally porous and crystalline. The particles are 20 nm in size showing their large surface. Lattice fringes show crystallinity of these nanostructures.

Transmission electron microscopy image for synthesis at temperature of 85°C showed that the particles synthesized are generally spherical-shaped, porous, and polycrystalline materials. The particle size was generally 5 nm in size. The SAED showed that the particles are polycrystalline considering that the diffraction is given in concentric circles.

3.3. Antimicrobial Activity of the Biogenic Au Nanoparticles. Antimicrobial activities of Au NPs from *Physalis peruviana* were studied for their antimicrobial activities as well as wound management. This was done to determine inhibition zones for gram-positive bacteria (*S. aureus* and *B. subtilis*) and gram-negative bacteria (*E. coli* and *P. aeruginosa)* as well as gram-positive fungus (*C. albicans*).

3.3.1. Analysis of the Microbial Activities. The analysis of the microbial activities was studied by determining the inhibition zones for the aqueous green gold nanoparticles. This was compared to those of the selected standard antibiotics. Table 1 shows minimum inhibition zones for aqueous green gold nanoparticles at different concentrations.

As the concentration of Au NPs increased, antimicrobial activity also increased due to a subsequent increase in interaction between Au NPs and the microbial cell wall. This may be attributed to generation of reactive oxygen species (ROS) [18]. Gold nanoparticles are usually not bactericidal at low concentrations but show higher bactericidal properties at relatively high concentrations [46, 47]. This may be attributed to the effect of coexisting chemicals, such as gold ions, surface coating agents, and chemicals involved in the synthesis that were not completely removed [46, 47]. In a study, higher concentration of CuO nanoparticles was required for a bactericidal effect to be achieved [48].

The antibacterial mechanism of Au NPs was associated to (i) the collapse in the membrane potential, hindering ATPase activity causing a deterioration of the cell metabolism and (ii) hindering the binding subunit of the ribosome to tRNA [49], and (iii) Shamaila et al. showed that Au NPs may affect the bacterial respiratory chain by attacking nicotinamide [50].

Comparison was also made between minimum inhibition zones using Au NPs at the concentration of 100 mM and that of aqueous *Physalis peruviana* extract. Table 2 shows the comparison of minimum inhibition zones of aqueous Au NPs at 100 mM with the aqueous *Physalis peruviana* extract. From Table 2, it is evident that the minimum inhibition zones varied significantly.

Gold nanoparticles can exert antibacterial activity through a multitude of mechanisms. This includes direct interaction of the Au NPs with the bacterial cell wall. The Au NPs inhibit respiratory enzymes such as cytochrome oxidases, malate, and succinate dehydrogenases. It has been reported that nanoparticles are capable of holding fast onto the bacterial cell membrane followed by penetration into the cytoplasm. Once in the cytoplasm, the Au^+ transverses via the ion channels leading to the ribosomes, in effect it leads to the death of cells as a result of denaturing and suppression of enzymes/proteins needed to produce energy. The Au^+ present in the nanoparticles are also capable of interacting with phosphorus and sulphur present in both DNA and RNA leading to the disruption of DNA and RNA functions as reported [51]. The Au NPs may also inhibit the formation of biofilm, triggers innate as well as adaptive host immune responses, generates reactive oxygen species, and induces interactions of the Au NPs with DNA and/or proteins. The fact that the mechanism of action of Au NPs against bacteria is different from known standards, they can be of great usefulness against multidrug-resistant (MDR) bacteria [35, 52]. Table 3 shows inhibition zones for standard antibiotics compared to Au NPs.

The antimicrobial activity of Au NPs against *E. coli* was comparable to those of amoxyclav, nitrofurantoin, nalidixic acid, gentamicin, sulphamethoxazole and ceftriaxone. However, when compared to norfloxacin and ofloxacin, its antimicrobial activity was lower but its antifungal activity was significantly higher or comparable to sulphamethoxazole and ofloxacin. As observed in Table 3, the microorganism under study demonstrated a significant level of resistance to the standards used in this study at the tested concentration. This activity was concentration dependent as when the nanoparticles were prepared using hydrochloroauric acid trihydrate of 100 mM, the activity was higher as more Au NPs were generated. As the concentration of Au NPs increased, antimicrobial activity increased due to a subsequent increase in interaction between Au NPs and the microbial cell wall due to generation of reactive oxygen species [18, 53]. Figure 5(a) shows the zones of inhibition of Au NP solution; Figure 5(b) shows the zones of inhibition for antibiotic standards, respectively.

3.3.2. In-Vivo Wound Healing Studies. The ability of Au NP coated sterile wound gauze to promote wound healing was evaluated using nude rabbits. Figure 6 shows macroscopic appearance of experimental wounds at various time intervals after surgery.

The rate of wound healing using Au NP coated sterile cotton gauze was faster as compared to the control cotton gauze and this trend was observed from the third day after application of the dressings on the wound area. On the 6^{th} day, re-epithelization in animals dressed with Au NP coated cotton gauze had already begun, while in the control group, hematoceles could still be observed. On the 14^{th} day, both the control group and the animals coated with Au NPs were observed to be completely healed which implies that Au NPs had good biocompatibility as signs of infection were not present. In addition, we had hypothesized that the antimicrobial activity of Au NPs effectively prevented the proliferation of microorganisms which accelerated tissue regeneration and healing.

Wound treated with the cotton gauze with Au NPs did not show the evidence of pus accumulation, fibrin deposition, polymorphonuclear cells infiltration, or edema in the lesions of the animal, but were seen in control and basal ointment groups as was observed in another study [54]. Accumulation and overactivation of lymphocytes, macrophages, and neutrophils in the wound site and their extreme secretion produced pus in the wound which reduced the healing process. Further, as reported elsewhere, the presence of free radicals may increase the amount of pus [54, 55]. The wound healed within the first 15 days and that is similar to the results in another study on wound healing using metal nanoparticles [56]. Endogenous collagen matrix may have supported tissue regeneration [57].

Table 1: Minimum inhibition zones for Au NPs of different concentrations synthesized from *Physalis peruviana*.

Samples	Conc. (mM)	Minimum inhibition zones (mean ± standard deviation) in mm				
		EC	PA	CA	BS	SA
Au NPs	100	19.0 ± 1.0^{A}	10.0 ± 1.0^{BA}	17.0 ± 1.0^{A}	17.0 ± 0.0^{A}	17.0 ± 1.0^{A}
	10	18.0 ± 1.0^{B}	11.0 ± 0.0^{A}	15.0 ± 1.0^{B}	16.0 ± 1.0^{B}	15.0 ± 1.0^{B}
	1	17.0 ± 1.0^{BC}	10.0 ± 1.0^{BA}	13.0 ± 0.0^{C}	14.0 ± 1.0^{C}	13.0 ± 0.0^{C}
	0.1	16.0 ± 1.0^{C}	9.0 ± 1.0^{B}	12.0 ± 1.0^{C}	15.0 ± 1.0^{C}	12.0 ± 1.0^{D}

*Values represent means ± Sd of triplicate analysis. *Means with different superscripts in the same column are significantly different at $p > 0.05$(data analysed by SAS). *Note.* Au NPs: gold nanoparticles; EC: *Escherichia coli*; CA: *Candida albicans*; PA: *Pseudomonas aeruginosa*; BS: *Bacillus subtilis;* SA: *Staphylococcus aureus*. The inhibition zones for Au NPs of different concentrations varied significantly between concentrations (one-way ANOVA at $P < 0.05$). The Au NPs showed antimicrobial activities at different concentrations with the mean inhibitory zone diameter of 16–19 mm in *E. coli*, 9–11 mm against *P. aeruginosa,* 12–17 mm against *C. albicans,* 14–17 mm against *B. subtilis,* and 12–17 mm against *S. aureus*. This activity was concentration-dependent and the inhibition zones against the microbes increased significantly with concentration, except for *P. aeruginosa* with minimum inhibition zone of 9 mm. The highest antibacterial activity was at 100 mM of Au NPs against EC, BS, and SA. The Au NPs were also effective against fungal infection based on the inhibition zone of *C. albicans* (17 mm).

Table 2: Comparison of minimum inhibition zones of aqueous Au NPs at 100 mM with the aqueous *Physalis peruviana* extract.

Sample	Conc.	Minimum inhibition zones (mean ± standard deviation) in mm				
		EC	PA	CA	BS	SA
Au NPs	100 mM	19.0 ± 1.0^{A}	10.0 ± 1.0^{A}	17.0 ± 1.0^{A}	17.0 ± 0.0^{A}	19.0 ± 0.0^{A}
Physalis peruviana extract	10^{0}	9.0 ± 1.0^{B}	10.0 ± 2.0^{A}	0.0 ± 0.0^{B}	7.0 ± 1.0^{B}	8.0 ± 1.0^{B}

*Values represent means ± Sd of triplicate analysis. *Means with different superscripts in the same column are significantly different at $p > 0.05$ (data analysed by SAS). The inhibition zones for Au NPs at the concentration of 100 mM and *Physalis peruviana* extract varied significantly in all the microbial cells, except for *P. aeruginosa* (one-way ANOVA, $F_{(3,11)} = 2.67$, $P = 0.1189$). The inhibition zone for Au NPs at the concentration of 100 mM varied significantly in the microbial cells of *E. coli* ($F_{(3,11)} = 2.67$, $P = 0.0306$), *C. albicans* ($F_{(3,11)} = 2.67$, $P = 0.0005$), *B. subtilis* ($F_{(3,11)} = 2.67$, $P = 0.0306$), and *S. aureus* ($F_{(3,11)} = 2.67$, $P = 0001$) which was highly significant. Antimicrobial activity exhibited by the Au NPs was significantly higher than that of the aqueous extract, implying that there was enhanced activity, as a result of incorporation of the gold ions.

Table 3: Inhibition zones for standard antibiotics compared to Au NPs.

		Minimum inhibition zones (mean ± standard deviation) in mm				
		SA	PA	BS	EC	CA
Au NPs		19.0 ± 0.0	10.0 ± 1.0	17.0 ± 0.0	19.0 ± 1.0	17.0 ± 1.0
Antibiotic standards	SX	8.00 ± 0.00	14.00 ± 0.00	12.00 ± 0.00	17.00 ± 1.00	9.00 ± 0.00
	GEN	8.00 ± 0.00	9.00 ± 0.00	8.00 ± 0.00	13.00 ± 0.00	NI
	AMC	9.00 ± 0.00	NI	8.00 ± 0.00	14.00 ± 0.00	NI
	NX	9.00 ± 3.00	14.00 ± 0.00	12.00 ± 0.00	28.00 ± 0.00	NI
	CTR	32.00 ± 1.00	9.00 ± 0.00	NI	25.00 ± 2.12	NI
	NIT	NI	NI	8.00 ± 0.00	12.00 ± 0.00	NI
	OF	NI	11.00 ± 0.00	9.00 ± 1.00	27.00 ± 3.00	12.00 ± 0.00
	NA	NI	NI	9.00 ± 0.00	15.00 ± 3.00	NI

Key: SX: sulphamethoxazole (25 μg); GEN: gentamycin (10 μg); AMC: amoxyclav (combination of amoxycillin and clavulanic acid, 20/10 μg, respectively); NX: norfloxacin (10 μg); CTR: ceftriaxone (30 μg); NIT: nitrofurantoin (200 μg); OF: ofloxacin (10 μg); NA: nalidixic acid (30 μg); NI: no inhibition; PA: *Pseudomonas aeruginosa*; BS: *Bacillus subtilis;* EC: *Escherichia coli*; CA: *Candida albicans;* SA: *Staphylococcus aureus.*

Mechanistically, in wound healing, Au NPs may adhere to the surface of bacterial cells by electrostatic interaction in the form of metallic gold which causes impairment of cell membrane, leakage of cell contents, and production of reactive oxygen species (ROS) [58]. Moreover, gold ions released may also tend to bind to thiol (sulfhydryl) groups of cellular lipoproteins to interfere with the respiratory chain and generate ROS [59]. In aerobic life of an organism, reactive oxygen species (ROS) are never welcome. These partial or activated derivatives of oxygen (singlet oxygen ($^1O_2$), superoxide anion (O_2^-), hydrogen peroxide (H_2O_2) and hydroxyl radical (HO)) are highly reactive and toxic, possible of causing oxidative destruction of cell components [60].

The effectiveness of ROS in damaging, as a protective or signaling factor, depends on the delicate equilibrium between ROS production and scavenging at the proper site of the cell and time [61]. When the rate of generation of ROS overweighs the rate at which ROS is scavenging, it leads to a harmful imbalance in the antioxidative system of the cell. This imbalance (often called as oxidative burst) results in widespread damage in cells including peroxidation of membrane lipids, oxidative damage to vital biomolecules such as nucleic acids and proteins, and also the activation of

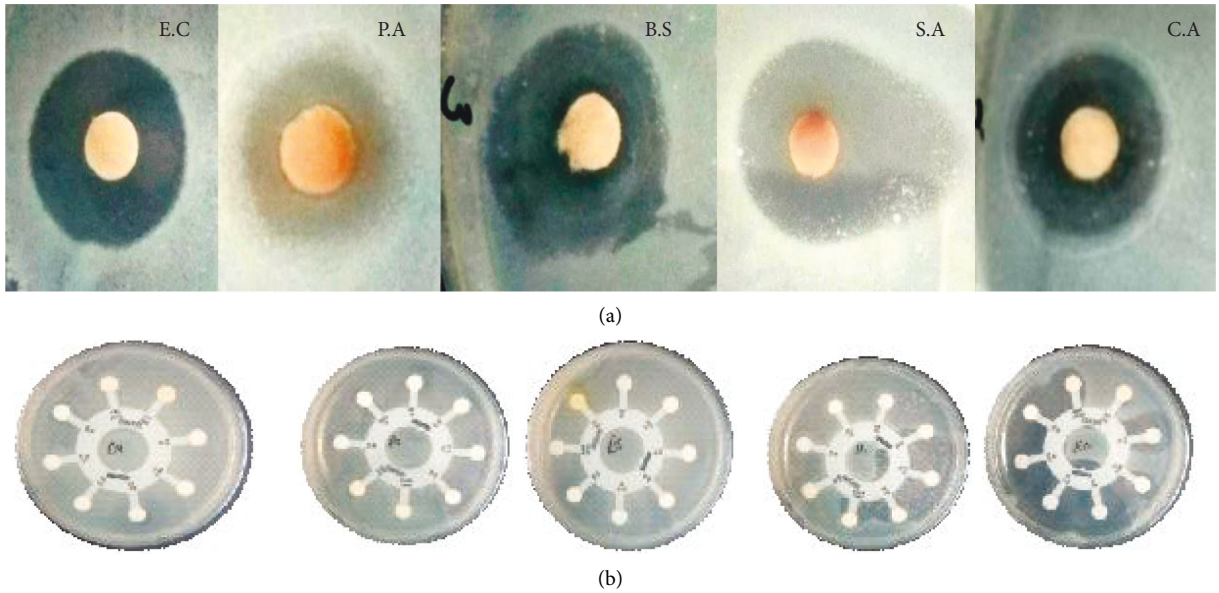

Figure 5: (a) Zone of inhibition of Au NP aqueous solution prepared using 100 mM Au^{+}. (b) Zone of inhibition of standard antibiotics.

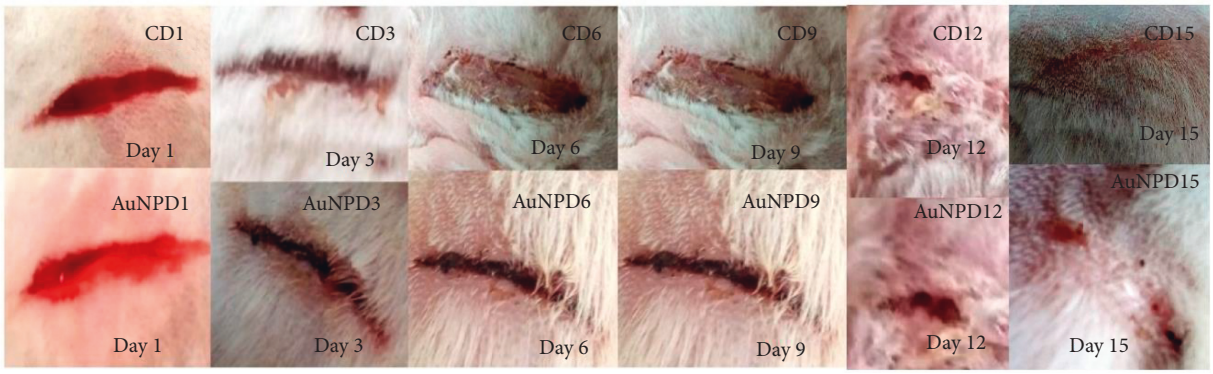

Figure 6: Macroscopic appearance of wounds at various time intervals. CD1, CD3, CD6, and CD9 show experimental wound appearances for control, on day one, three, six, and nine, respectively. AuNPD1, AuNPD3, AuNPD6, and AuNPD9 show wound appearance when treated with Au NPs on day one, three, six, and nine, respectively.

programmed cell death (PCD) pathway probably making it possible for the NPs to initiate membrane lipid peroxidation. Consequently, the disintegration of membranes then facilitates the entrance of metals and NPs. However, as reported by [59], changes, including collagen content, epithelial thickness, and related growth factors, cannot be determined by the external phase.

4. Conclusion

In this study, aqueous leaf extract of *Physalis peruviana* was found to successfully synthesize gold nanoparticles at room temperature as well as at varied temperatures (25°C to 85°C). The synthesized Au NPs, DLS, and zeta potential analysis showed that the polydispersity index was high and this was attributed to the heterogeneity of the chemical components of the plants. The Au NPs synthesized from *Physalis peruviana* plant extract were likely to be anisotropic in shape and size. This was shown from the UV-Vis spectra and confirmed by the TEM images obtained. The Au NPs are porous and have a hollow structure. The grain boundaries are of size 10 nm. The particles are also crystalline and the small lattice is due to the small grains. The gold nanoparticles have been found to have a higher antibacterial and antifungal activity compared to plant extract. Study on the wound healing efficacy of the plant was also positive with the incision healing within 14 days showing positivity towards wound management by the biogenically synthesized gold nanoparticles.

Data Availability

The authors confirm that the data supporting the findings of the study are available within the article. Raw data that support the findings of the study are available from corresponding author upon request.

Conflicts of Interest

The authors declare no conflicts of interest.

Acknowledgments

The authors would like to thank the National Commission for Science, Technology and Innovation (NACOSTI/RCD/ST&1/7THCALL/PhD/041), Kenya, for the research funding support. The authors also acknowledge the support of the Jomo Kenyatta University of Science and Technology through Dr. Edwin Madivoli and University of Western Cape for allowing them to use their facilities for research. The authors sincerely thank Prof. Oyaro of Masai Mara University for the enormous support he granted in this study. The support received from Prof. Madiehe, Dr. Nicole, Ms. Amanda, and Ms. Koena, all of the University of the Western Cape, particularly in synthesis and characterization of the gold nanoparticles, was not in vain and hence appreciated.

Supplementary Materials

Ethical Review process. A proposal this article was prepared and submitted to the Ethical Review Committee at Jaramogi Oginga Odinga University of Science and Technology (JOOUST). The ethical review number at JOOUST is ERC/29/4/22-25 (Appendix 1). The subsequent research permit from National Commission for Science, Technology and Innovation, Kenya identification license number: NACOSTI/P/22/18037 (Appendix 2). The recommended small animal handling certificate by the ethical review committee was done at Jomo Kenyatta University of Agriculture and Technology (Appendix 3). Appendix 1: Ethical Review certificate for the proposal: Biogenic Synthesis of Gold Nanoparticles from Physalis Peruviana and Application in Wound Healing. Appendix 2: Research license from National Commission for Science, Technology and Innovation, Kenya for the proposal: Biogenic Synthesis of Gold Nanoparticles from Physalis Peruviana and Application in Wound Healing. Appendix 3: The recommended small animal handling certificate by the ethical review committee at JOOUST for the proposal: Biogenic Synthesis of Gold Nanoparticles from Physalis Peruviana and Application in Wound Healing. (*Supplementary Materials*)

References

[1] R. Xu, G. Luo, H. Xia et al., "Novel bilayer wound dressing composed of silicone rubber with particular micropores enhanced wound re-epithelialization and contraction," *Biomaterials*, vol. 40, pp. 1–11, 2015.

[2] K. G. Harding, H. L. Morris, and G. K. Patel, "Science, medicine and the future: healing chronic wounds," *British Medical Journal*, vol. 324, no. 7330, pp. 160–163, 2002.

[3] WiseGuyReports, *Global Wound Care Market with Focus on Advanced Wound Care: Industry Analysis and Outlook*, 2017, https://www.grandviewresearch.com/industry-analysis/advanced-wound-care-market.

[4] N. Singh, D. G. Armstrong, and B. A. Lipsky, "Preventing foot ulcers in patients with diabetes," *Journal of the American Medical Association*, vol. 293, no. 2, pp. 217–228, 2005.

[5] M. C. Robson, D. L. Steed, and M. G. Franz, "Wound healing: biologic features and approaches to maximize healing trajectories," *Current Problems in Surgery*, vol. 38, no. 2, pp. A1–A140, 2001.

[6] M. Ovais, I. Ahmad, A. T. Khalil et al., "Wound healing applications of biogenic colloidal silver and gold nanoparticles: recent trends and future prospects," *Applied Microbiology and Biotechnology*, vol. 102, pp. 4305–4318, 2018.

[7] S. A. Eming, P. Martin, and M. Tomic-Canic, "Wound repair and regeneration: mechanisms, signaling, and translation," *Science Translational Medicine*, vol. 6, no. 265, pp. 265sr6-266, 2014.

[8] M. A. Fonder, G. S. Lazarus, D. A. Cowan, B. Aronson-Cook, A. R. Kohli, and A. J. Mamelak, "Treating the chronic wound: a practical approach to the care of nonhealing wounds and wound care dressings," *Journal of the American Academy of Dermatology*, vol. 58, no. 2, pp. 185–206, 2008.

[9] P. G. Bowler, "Wound pathophysiology, infection and therapeutic options," *Annals of Medicine*, vol. 34, no. 6, pp. 419–427, 2002.

[10] K. F. Cutting, "Wound dressings: 21st century performance requirements," *Journal of Wound Care*, vol. 19, no. Sup1, pp. 4–9, 2010.

[11] O. V. Salata, "Applications of nanoparticles in biology and medicine," *Journal of Nanobiotechnology*, vol. 2, no. 1, pp. 3–6, 2004.

[12] M. Mahdavi, F. Namvar, M. Ahmad, and R. Mohamad, "Green biosynthesis and characterization of magnetic iron oxide (Fe3O4) nanoparticles using seaweed (Sargassum muticum) aqueous extract," *Molecules*, vol. 18, no. 5, pp. 5954–5964, 2013.

[13] P. Raveendran, J. Fu, and S. L. Wallen, "A simple and "green" method for the synthesis of Au, Ag, and Au-Ag alloy nanoparticles," *Green Chemistry*, vol. 8, no. 1, pp. 34–38, 2006.

[14] M. Singh, S. Manikandan, and A. K. Kumaraguru, "Nanoparticles: a new technology with wide applications," *Research Journal of Nanoscience and Nanotechnology*, vol. 1, pp. 1–11, 2011.

[15] K. Niska, E. Zielinska, M. W. Radomski, and I. Inkielewicz-Stepniak, "Metal nanoparticles in dermatology and cosmetology: interactions with human skin cells," *Chemico-Biological Interactions*, vol. 295, pp. 38–51, 2018.

[16] I. Kalashnikova, S. Das, and S. Seal, "Nanomaterials for wound healing: scope and advancement," *Nanomedicine*, vol. 10, no. 16, pp. 2593–2612, 2015.

[17] M. G. Arafa and R. F. El-Kased, "Thermoresponsive gels containing gold nanoparticles as smart antibacterial and wound healing agents," *Scientific Reports*, vol. 8, pp. 13674–13678, 2018.

[18] V. Vijayakumar, S. K. Samal, S. Mohanty, and S. K. Nayak, "Recent advancements in biopolymer and metal nanoparticle-based materials in diabetic wound healing management," *International Journal of Biological Macromolecules*, vol. 122, pp. 137–148, 2019.

[19] A. Panacek, M. Kolar, R. Vecerova et al., "Antifungal activity of silver nanoparticles against Candida spp," *Biomaterials*, vol. 30, no. 31, pp. 6333–6340, 2009.

[20] S. Ray, R. Mohan, J. K. Singh et al., "Anticancer and antimicrobial metallopharmaceutical agents based on palladium, gold, and silver N-heterocyclic carbene complexes," *Journal of*

the American Chemical Society, vol. 129, no. 48, pp. 15042–15053, 2007.

[21] Government of Kenya, *Siaya County Integrated Development 2013-2017*, Government Printers, Nairobi, Kenya, 2013.

[22] A. Kumar, Y. Chisti, and U. Chand, "Synthesis of metallic nanoparticles using plant extracts," *Biotechnology Advances*, vol. 31, pp. 346–356, 2013.

[23] A. W. Bauer, W. M. M. Kirby, J. C. Sherris, and M. Turck, "Antibiotic susceptibility testing by a standardized single disk method," *American Journal of Clinical Pathology*, vol. 45, pp. 493–496, 1966.

[24] M. R. S. Zaidan, A. Noor Rain, A. R. Badrul, A. Adlin, A. Norazah, and I. Zakiah, "In vitro screening of five local medicinal plants for antibacterial activity using disc diffusion method," *Tropical Biomedicine*, vol. 22, no. 2, pp. 165–170, 2005.

[25] E. S. Madivoli, E. G. Maina, P. K. Kairigo et al., "In vitro antioxidant and antimicrobial activity of Prunus africana (Hook. f.) Kalkman (bark extracts) and Harrisonia abyssinica Oliv. extracts (bark extracts): a comparative study," *Journal of Medicinal Plants for Economic Development*, vol. 2, no. 1, pp. 1–9, 2018.

[26] P. Orlowski, M. Zmigrodzka, E. Tomaszewska et al., "Polyphenol-conjugated bimetallic Au@AgNPs for improved wound healing," *International Journal of Nanomedicine*, vol. 15, pp. 4969–4990, 2020.

[27] S. Ghosh, S. Patil, M. Ahire et al., "Synthesis of gold nanoanisotrops using Dioscorea Bulbifera tuber extract," *Journal of Nanomaterials*, vol. 2011, pp. 1–8, 2011.

[28] D. Khatri and S. B. B. Chhetri, "Reducing sugar, total phenolic content, and antioxidant potential of Nepalese plants," *BioMed Research International*, vol. 2020, pp. 1–7, 2020.

[29] E.-Y. Kim, S.-K. Ham, M. K. Shigenaga, and O. Han, "Bioactive dietary polyphenolic compounds reduce nonheme iron transport across human intestinal cell monolayers," *Journal of Nutrition*, vol. 138, no. 9, pp. 1647–1651, 2008.

[30] M. N. Nadagouda and R. S. Varma, "Green synthesis of silver and palladium nanoparticles at room temperature using coffee and tea extract," *Green Chemistry*, vol. 10, no. 8, pp. 859–862, 2008.

[31] E. Porcel, S. Liehn, H. Remita et al., "Platinum nanoparticles: a promising material for future cancer therapy?" *Nanotechnology*, vol. 21, no. 8, pp. 085103–103, 2010.

[32] G. Rastogi, A. Sbodio, J. J. Tech, T. V. Suslow, G. L. Coaker, and J. H. J. Leveau, "Leaf microbiota in an agroecosystem: spatiotemporal variation in bacterial community composition on field-grown lettuce," *The ISME Journal*, vol. 6, no. 10, pp. 1812–1822, 2012.

[33] P. K. Jain, K. S. Lee, I. H. El-Sayed, and M. A. El Sayed, "Calculated absorption and scattering properties of gold nanoparticles of different size, shape, and composition: applications in biological imaging and biomedicine," *The Journal of Physical Chemistry B*, vol. 110, no. 14, pp. 7238–7248, 2006.

[34] L. Guo, J. A. Jackman, H. H. Yang, P. Chen, N. J. Cho, and D. H. Kim, "Strategies for enhancing the sensitivity of plasmonic nanosensors," *Nano Today*, vol. 10, no. 2, pp. 213–239, 2015.

[35] K. S. Siddiqi, A. Husen, and R. A. K. Rao, "A review on biosynthesis of silver nanoparticles and their biocidal properties," *Journal of Nanobiotechnology*, vol. 16, no. 1, pp. 14–18, 2018.

[36] K. D. Arunachalam and S. K. Annamalai, "Chrysopogon zizanioides aqueous extract mediated synthesis, characterization of crystalline silver and gold nanoparticles for biomedical applications," *International Journal of Nanomedicine*, vol. 8, pp. 2375–2384, 2013.

[37] A. O. Nyabola, P. G. Kareru, E. S. Madivoli, S. I. Wanakai, and E. G. Maina, "formation of silver nanoparticles via aspilia pluriseta extracts their antimicrobial and catalytic activity," *Journal of Inorganic and Organometallic Polymers and Materials*, vol. 30, no. 9, pp. 3493–3501, 2020.

[38] P. Mulvaney, "Surface plasmon spectroscopy of nanosized metal particles," *Langmuir*, vol. 12, no. 3, pp. 788–800, 1996.

[39] A. M. K. Anwar, M. Mady, and M. Ghannam, "Physical properties of different gold nanoparticles: ultraviolet-visible and fluorescence measurements," *Journal of Nanomedicine & Nanotechnology*, vol. 3, no. 3, pp. 178–194, 2012.

[40] A. A. Elbagory, C. N. Cupido, M. Meyer, and A. A. Hussein, "Large scale screening of Southern African plant extracts for the green synthesis of gold nanoparticles using microtitre-plate method," *Molecules*, vol. 21, no. 11, pp. 1498–1524, 2016.

[41] V. Borse and A. N. Konwar, "Synthesis and characterization of gold nanoparticles as a sensing tool for the lateral flow immunoassay development," *Sensors International*, vol. 1, Article ID 100051, 2020.

[42] K. Chandran, S. Song, and S. I. Yun, "Effect of size and shape controlled biogenic synthesis of gold nanoparticles and their mode of interactions against food borne bacterial pathogens," *Arabian Journal of Chemistry*, vol. 12, no. 8, pp. 1994–2006, 2019.

[43] V. V. Makarov, A. J. Love, O. V. Sinitsyna et al., "Green" nanotechnologies: synthesis of metal nanoparticles using plants," *Acta Naturae*, vol. 6, no. 1, pp. 35–44, 2014.

[44] T. Zheng, S. Bott, and Q. Huo, "Techniques for accurate sizing of gold nanoparticles using dynamic light scattering with particular application to chemical and biological sensing based on aggregate formation," *ACS Applied Materials & Interfaces*, vol. 8, no. 33, pp. 21585–21594, 2016.

[45] W. Chen, W. Cai, L. Zhang, G. Wang, and L. Zhang, "Sonochemical processes and formation of Gold nanoparticles within pores of mesoporous Silica," *Journal of Colloid and Interface Science*, vol. 238, no. 2, pp. 291–295, 2001.

[46] T. P. Shareena Dasari, Y. Zhang, and H. Yu, "Antibacterial activity and cytotoxicity of gold (I) and (III) ions and gold nanoparticles," *Biochemistry & Pharmacology: Open Access*, vol. 4, no. 6, pp. 199–206, 2015.

[47] Y. Zhang, T. P. Shareena Dasari, H. Deng, and H. Yu, "Antimicrobial activity of gold nanoparticles and ionic gold," *Journal of Environmental Science and Health, Part C*, vol. 33, no. 3, pp. 286–327, 2015.

[48] G. Ren, D. Hu, E. W. C. Cheng, M. A. Vargas-Reus, P. Reip, and R. P. Allaker, "Characterisation of copper oxide nanoparticles for antimicrobial applications," *International Journal of Antimicrobial Agents*, vol. 33, no. 6, pp. 587–590, 2009.

[49] Y. Cui, Y. Zhao, Y. Tian, W. Zhang, X. Lu, and X. Jiang, "The molecular mechanism of action of bactericidal gold nanoparticles on *Escherichia coli*," *Biomaterials*, vol. 33, no. 7, pp. 2327–2333, 2012.

[50] S. Shamaila, N. Zafar, S. Riaz, R. Sharif, J. Nazir, and S. Naseem, "Gold nanoparticles: an efficient antimicrobial agent against enteric bacterial human pathogen," *Nanomaterials*, vol. 6, no. 4, pp. 71–78, 2016.

[51] M. Parthibavarman, S. Bhuvaneshwari, M. Jayashree, and R. BoopathiRaja, "Green synthesis of silver (Ag) nanoparticles using extract of apple and grape and with enhanced visible

light photocatalytic activity," *Bionanoscience*, vol. 9, no. 2, pp. 423–432, 2019.

[52] A. Bassegoda, K. Ivanova, E. Ramon, and T. Tzanov, "Strategies to prevent the occurrence of resistance against antibiotics by using advanced materials," *Applied Microbiology and Biotechnology*, vol. 102, no. 5, pp. 2075–2089, 2018.

[53] M. Arakha, S. Pal, D. Samantarrai et al., "Antimicrobial activity of iron oxide nanoparticle upon modulation of nanoparticle-bacteria interface," *Scientific Reports*, vol. 5, no. 1, p. 14813, 2015.

[54] D. Foschi, E. Trabucchi, M. Musazzi et al., "The effects of oxygen free radicals on wound healing," *International Journal of Tissue Reactions*, vol. 1, no. 10, 1988.

[55] T. J. Koh and L. A. DiPietro, "Inflammation and wound healing: the role of the macrophage," *Expert Reviews in Molecular Medicine*, vol. 13, pp. e23–13, 2011.

[56] T. Shanmugasundaram, M. Radhakrishnan, V. Gopikrishnan, K. Kadirvelu, and R. Balagurunathan, "In vitro antimicrobial and in vivo wound healing effect of actinobacterially synthesised nanoparticles of silver, gold and their alloy," *RSC Advances*, vol. 7, no. 81, pp. 51729–51743, 2017.

[57] A. R. Fernandes, I. Mendonça-Martins, M. F. A. Santos et al., "Improving the anti-inflammatory response via gold nanoparticle vectorization of CO-releasing molecules," *ACS Biomaterials Science & Engineering*, vol. 6, no. 2, pp. 1090–1101, 2020.

[58] X. Hu, A. Ahmeda, and M. M. Zangeneh, "Chemical characterization and evaluation of antimicrobial and cutaneous wound healing potentials of gold nanoparticles using allium saralicum RM fritsch," *Applied Organometallic Chemistry*, CAS, vol. 34, no. 4, , p. e5484, 2020.

[59] K. Wang, H. Wang, S. Pan et al., "Evaluation of new film based on chitosan/gold nanocomposites on antibacterial property and wound-healing efficacy," *Advances in Materials Science and Engineering*, vol. 2020, Article ID 6212540, 10 pages, 2020.

[60] K. Asada and M. Takahashi, "Production and scavenging of active oxygen radicals in photosynthesis," *Photoinhibition, 9*, pp. 227–288, Elsevier, Amsterdam, Netherlands, 1987.

[61] P. L. Gratão, A. Polle, P. J. Lea, and R. A. Azevedo, "Making the life of heavy metal-stressed plants a little easier," *Functional Plant Biology*, vol. 32, no. 6, pp. 481–494, 2005.